The American Journal of Pathology, Vol. 190, No. 4, April 2020

ELSEVIER

The American Journal of PATHOLOGY

ajp.amjpathol.org

GASTROINTESTINAL, HEPATOBILIARY, AND PANCREATIC PATHOLOGY

mTORC2 Signaling Is Necessary for Timely Liver Regeneration after Partial Hepatectomy

Meng Xu,[*†] Haichuan Wang,[‡†§*] Jingxiao Wang,[†¶] Deviana Burhan,[‖] Runze Shang,[†**] Pan Wang,[†,††] Yi Zhou,[†‡‡] Rong Li,[§§] Bingyong Liang,[†¶¶] Katja Evert,[‖‖] Kirsten Utpatel,[‖‖] Zhong Xu,[***] Xinhua Song,[†] Li Che,[†] Diego F. Calvisi,[‖‖] Bruce Wang,[‖] Xi Chen,[*] Yong Zeng,[‡§] and Xin Chen[†]

From the Departments of General Surgery and Anesthesiology,[§§] The Second Hospital of Xi'an Jiaotong University, and the Department of Infectious Diseases,[‡‡] The First Affiliated Hospital of Xi'an Jiaotong University, Xi'an Jiaotong University, Xi'an, PR China; the Department of Liver Surgery,[‡] Liver Transplantation Division, and the Laboratory of Liver Surgery,[§] West China Hospital, Sichuan University, Chengdu, PR China; the Departments of Bioengineering and Therapeutic Sciences,[†] and Medicine,[‖] Liver Center, University of California, San Francisco, California; the School of Life Sciences,[¶] Beijing University of Chinese Medicine, Beijing, PR China; the Department of Hepatobiliary Surgery,[**] Xijing Hospital, Air Force Military Medical University, Xi'an, PR China; the Beijing Advanced Innovation Center for Food Nutrition and Human Health,[††] College of Food Science and Nutritional Engineering, Beijing, PR China; the Hepatic Surgery Center,[¶¶] Department of Surgery, Tongji Hospital, Tongji Medical College, Huazhong University of Science and Technology, Wuhan, PR China; the Institute of Pathology,[‖‖] University of Regensburg, Regensburg, Germany; and the Department of Gastroenterology,[***] Guizhou Provincial People's Hospital, Medical College of Guizhou University, Guiyang, PR China*

Accepted for publication December 5, 2019.

Address correspondence to Yong Zeng, M.D., Ph.D., Department of Liver Surgery, Liver Transplantation Division, West China Hospital, Sichuan University, No. 37, Guo Xue Xiang, Chengdu, Sichuan 610041, China; or Xin Chen, Ph.D., Department of Bioengineering and Therapeutic Sciences, University of California, San Francisco, 513 Parnassus Ave., San Francisco, CA 94143. E-mail: zengyong@medmail.com.cn or xin.chen@ucsf.edu.

Liver regeneration is a fundamental biological process required for sustaining body homeostasis and restoring liver function after injury. Emerging evidence demonstrates that cytokines, growth factors, and multiple signaling pathways contribute to liver regeneration. Mammalian target of rapamycin complex 2 (mTORC2) regulates cell metabolism, proliferation and survival. The major substrates for mTORC2 are the AGC family members of kinases, including AKT, SGK, and PKC-α. We investigated the functional roles of mTORC2 during liver regeneration. Partial hepatectomy (PHx) was performed in liver-specific *Rictor* (the pivotal unit of mTORC2 complex) knockout ($Rictor^{LKO}$) and wild-type ($Rictor^{fl/fl}$) mice. *Rictor*-deficient mice were found to be more intolerant to PHx and displayed higher mortality after PHx. Mechanistically, loss of Rictor resulted in decreased Akt phosphorylation, leading to a delay in hepatocyte proliferation and lipid droplets formation along liver regeneration. Overall, these results indicate an essential role of the mTORC2 signaling pathway during liver regeneration. *(Am J Pathol 2020, 190: 817–829; https://doi.org/10.1016/j.ajpath.2019.12.010)*

The liver is a vital organ and possesses multiple essential functions for regulating metabolism of other tissues in the body, including detoxification, decomposition, synthetization, digestion, and storage.[1,2] Regeneration after injury or surgical resection is a unique capacity of the liver.[3,4] It has been reported that healthy liver can regenerate back to its full size from as little as 25% of the original liver mass.[5] Consequently, partial hepatectomy (PHx) and liver transplantation are widely performed among patients with various liver diseases.[6] However, clinical scenarios of patients with liver dysfunction are more complicated, and regeneration processes in unhealthy livers are simultaneously affected by other complications. Indications for these procedures tightly depend on liver remnant regeneration potential. Furthermore, no therapeutic strategies to accelerate liver regeneration exist.[7] Thus, a better understanding of the mechanisms

Supported by NIH grants R01CA136606 (X.C.), R01CA204586 (X.C.), P30DK026743 (University of California, San Francisco Liver Center), and K08DK101603 (B.W.); the Burroughs Wellcome Fund Career Award for Medical Scientists (B.W.); China Scholarship Council contracts 201706240075 (P.W.) and 201703170154 (R.S.); National Natural Science Foundation of China grant 81902449 (M.X.); and West China Hospital, Sichuan University, Post-Doctoral Research Project funds (H.W.); and in part by the NIH Diabetes Research Center grant P30 DK063720.

M.X. and H.W. contributed equally to this work.

Disclosures: None declared.

https://doi.org/10.1016/j.ajpath.2019.12.010

whereby liver regeneration occurs would be highly beneficial for tackling these issues.

Described >80 years ago, the two-thirds PHx remains the state-of-the-art method for the in-depth analysis of signaling pathways involved in liver regeneration.[8,9] After PHx, the remaining liver lobes are able to regenerate and completely replace the missing parenchyma, with consequent morphologic recovery and functional restoration.[10] In this process, hepatocytes replicate first, followed by proliferation of biliary epithelia cells and sinusoidal endothelial cells. Meanwhile, newly divided cells undergo restructuring, angiogenesis, and reformation of extracellular matrix to structurally recover from PHx.[11] Simultaneously, with a series of intrinsic regulations, liver function recovers to maintain the body homeostasis. In mice, it takes approximately 1 week for the liver to fully regenerate after PHx.

Several signaling pathways are involved in liver regeneration, including growth factors, cytokines, hormones, and many transcription factors. Among them, mammalian target of rapamycin (mTOR) signaling is one of the well-known pathways to be involved in liver regeneration.[12] mTOR kinases include two distinct protein complexes with specific binding partners, consisting of regulatory-associated protein of mTOR (Raptor) in mTOR complex 1 (mTORC1) and rapamycin-insensitive companion of mTOR (Rictor) in mTOR complex 2 (mTORC2). mTORC2 regulates Akt, Sgk, and Pkc (AGC) kinases, which are essential for organismal development and viability in response to nutrient availability.[13] Akt kinases are considered to be the major substrates for mTORC2; once activated, mTORC2 phosphorylates Akt kinases at the S473 (for Akt1) or S474 (for Akt2) position, which is required for their activation. In mammals, there are three Akt isoforms, namely, Akt1, Akt2, and Akt3. Although Akt1 and Akt2 are expressed in the liver, Akt3 is predominantly expressed in the brain. Akt2 comprises approximately 85% of total Akt in the liver and is the major Akt isoform downstream of insulin receptors in regulating glucose and fatty acid catabolism.[14]

Mounting evidence indicates the key roles of mTOR signaling during liver regeneration.[12,15] Studies have found that the phosphatidylinositol 3-kinase (PI3K)/AKT/mTOR pathway is activated after PHx.[16–18] mTOR phosphorylates S6K1 and is required for the expression of cyclin D1 during liver regeneration.[19] Treatment with rapamycin, an mTORC1 inhibitor, after PHx leads to decreased hepatocyte proliferation and increased apoptosis.[20,21] In addition, recent studies have found that ablation of *Akt1* or *Akt2* alone does not influence liver regeneration after PHx in mice, whereas combined loss of *Akt1* and *Akt2* isoforms leads to impaired regeneration and increased mortality. Intriguingly, simultaneous deletion of *FoxO1* in the liver rescued the survival defects of *Akt1* and *Akt2* double knockout (KO) mice.[22] Altogether, this body of information implies pivotal function of Akt in liver development and regeneration. However, because Akt regulates several proteins and signaling cascades, the specific requirement of mTORC2 in this process and whether Akt activation is required during liver regeneration remain poorly defined.

To better delineate the role of mTORC2 along liver regeneration, two-thirds PHx was performed in liver-specific *Rictor* KO ($Rictor^{LKO}$) mice and wild-type (WT) mice. $Rictor^{LKO}$ mice were found to be more intolerant to PHx, having a lower survival rate than WT mice. Moreover, delayed cell proliferation and lipid droplets formation as well as cell cycle arrest were observed in $Rictor^{LKO}$ mice. Therefore, our findings highlight the role of mTORC2 signaling in lipid formation and cell proliferation during liver regeneration.

Materials and Methods

Animals

Albumin-Cre[23] and $Rictor^{flox/flox}$ mice[24] (all in the C57BL/6 background) were purchased from Jackson Laboratory (Bar Harbor, ME) and then crossed to generate *Albumin-Cre*$^{+}$ $Rictor^{flox/flox}$ ($Rictor^{LKO}$) and *Albumin-Cre*$^{-}$ $Rictor^{flox/flox}$ mice ($Rictor^{fl/fl}$). Mice were sacrificed at 3, 5, and 8 weeks of age for the liver development study. For the liver regeneration study, two-thirds PHx was performed in 8-week−old male mice. Genotyping was conducted using a Mouse Direct PCR Kit (catalog number B40015; Bimake, Houston, TX) according to the standard protocol. The primers used were as follows: common reverse, 5′-CCTGCCAGCCATGGATATAA-3′; mutant forward, 5′-GAAGCAGAAGCTTAGGAAGATGG-3′; wild-type forward, 5′-GTTGTCCTTCTTTGTGCTGA-3′. Animal experiments were performed according to protocols approved by the Committee for Animal Research at the University of California, San Francisco (San Francisco, CA).

PHx Model

PHx was performed according to the technique described by Mitchell and Willenbring.[25] In brief, two-thirds of the liver (consisting of median and left lobes) was removed. The two-thirds PHx and sham surgery operation were performed under isoflurane (Sigma-Aldrich, St. Louis, MO) anesthesia. After PHx, mice were sacrificed at different time points: 1 to 7 days. The sham group was used as internal control. The regenerated liver was weighed, and the liver/body weight ratio was calculated. Liver tissues and blood samples were collected and analyzed as previously described.[26]

Histologic and Immunohistochemical Analysis

Tissue samples were fixed with 10% neutral buffered formalin (catalog number 5701; Thermo Fisher Scientific, Waltham, MA) at 4°C overnight, followed by paraffin embedding. Tissue blocks were trimmed and cut at a thickness of 5 μm. Antigen retrieval was conducted by boiling slides for 10 minutes with sodium citrate buffer (pH 6.0). Then the slides were blocked with the goat serum/ phosphate-buffered

saline (PBS) solution (1:20). Endogenous biotin, biotin receptors, and avidin-binding sites present in tissues were mocked with the Avidin/Biotin blocking kit (catalog number SP2001; Vector Laboratories, Burlingame, CA). After three washing steps in PBS, the tissue sections were then incubated with designated primary antibodies at 4°C overnight. The next day, slides were washed in PBS, and then endogenous peroxidase was blocked by 3% hydrogen peroxide at room temperature for 10 minutes. Subsequently, slides were incubated with the biotin conjugated secondary antibody (1:500; catalog number B2770; Thermo Fisher Scientific, Waltham, MA) for 30 minutes. The antibody was used according to the manufacturers and dilution for immunohistochemical analysis. After washing with PBS, the immunostaining signals were visualized using the Vectastain Elite ABC Kit (catalog number PK6100; Vector Laboratories, Burlingame, CA) and ImmPACT DAB EqV Peroxidase Substrate (catalog number SK4103; Vector Laboratories). Ki-67 and phosphorylated histone 3 (PH3) (Table 1) staining were quantified by using ImageJ software version 1.8.0 (NIH, Bethesda, MD; *http://imagej.nih.gov/ij*) and Image Pro Plus 7 software (Media Cybernetics, Rockville, MD).

Oil Red O and Periodic Acid-Schiff Staining

Liver tissues were embedded in optimum cutting temperature compound (Tissue-Tek, Sakura Finetek, Torrance, CA) and frozen in cold 2-methylbutane at −80°C. Frozen sections were cut at 5 μm in thickness. Oil Red O (catalog number KTORO; American MasterTech Scientific Laboratory Supplies, Lodi, CA) and periodic acid-Schiff (catalog number 22110645; Thermo Fisher Scientific) staining was performed on frozen sections according to the standard instructions.

Protein Extraction and Western Blot Analysis

Frozen mouse liver tissues were homogenized and lysed by applying M-PER Mammalian Protein Extraction Reagent (catalog number 78501; Thermo Fisher Scientific). A Bio-Rad Protein Assay Kit (Bio-Rad, Hercules, CA) was used to determine protein concentration according to the protocol of the manufacturer. Protein lysates (25 μg) were denatured and separated by SDS-PAGE. Nonspecific proteins on transferred membranes were blocked with a nonfat dry milk and tris-buffered saline with Tween 20 solution (1:20) for 1 hour and incubated with specific primary antibodies (Table 2) at 4°C overnight. After washing in tris-buffered saline with Tween 20 for 10 minutes three times, anti-mouse or anti-rabbit horseradish peroxidase secondary antibody (1:5000) was applied. Protein expression was detected with Super Signal West Pico Chemiluminescent Substrate (Pierce Chemical Co., New York, NY).

Table 1 Antibody Information for Immunohistochemistry

Antibody	Concentration	Manufacturer	Catalog number
Ki-67	1:150	Thermo Fisher Scientific	RM-9106-S1
Phosphorylated -histone H3 (Ser10)	1:100	Cell Signaling Technology	9701

Biochemical Assays

For glucose measurement, blood was collected in test strips and directly measured in a glucometer (Accu-Chek Active, Roche Diagnostics, Mannheim, Germany). Other blood biochemical indicators were sent and analyzed by the Zuckerberg San Francisco General Hospital Clinical Lab.

Hepatocyte Ploidy Analysis

Primary mouse hepatocytes were isolated using a two-step collagenase perfusion as previously described.[27] Before perfusion, a single lobe was ligated and collected for histologic analysis. Hepatocytes were separated from non-parenchymal cells using slow spin centrifugation and passed through a 70-μm cell strainer before purification through 50% equilibrated Percoll (GE Healthcare Biosciences, Marlborough, MA). Isolated hepatocytes were resuspended in Williams E Medium (Gibco, Waltham, MA) supplemented with GlutaMAX (Gibco), nonessential amino acids (Gibco), penicillin-streptomycin (Corning Inc., Corning, NY), and fetal bovine serum. Hepatocyte ploidy staining was performed as previously described.[28] Briefly, cells in suspension were stained with 15 μg/mL of Hoechst (catalog number 33342; Invitrogen, Carlsbad, CA), and 5 μmol/L of reserpine (Sigma-Aldrich) at 37°C for 30 minutes. After initial incubation, 5 μg/mL of propidium iodide was added to the cells and kept in ice. DNA content of labeled live cells was measured by flow cytometer (LSR II; BD, Franklin Lakes, NJ). Acquired data were analyzed by FACSDiva software version 8.0 (BD) and FlowJo software version 10 (BD).

RNA Sequencing and Data Analysis

Experimental design consisted of six groups: WT0D, WT2D, WT4D, KO0D, KO2D, and KO4D. WT represents WT *Rictor*$^{fl/fl}$ liver samples, whereas KO represents liver samples from *Rictor*^{LKO} mice. Each group had two biological replicates. RNA was isolated from liver tissues using Zymo quick-RNA miniprep kit (catalog number D7001; Zymo Research, Irvine, CA). RNA was quantified by nanodrop. RNA quality control was conducted with Bioanalyzer (Aligent, Santa Clara, CA). Library preparation and sequencing were performed by Novogene (Sacramento, CA). Gene read counts were in Ensembl ID and converted

Table 2 Antibody Information Western Blotting

Antibody	Concentration	Manufacturer	Catalog number
Rictor	1:500	Cell Signaling Technology	9476
p-AKT (Ser473)	1:1000	Cell Signaling Technology	3787
Total AKT	1:1000	Cell Signaling Technology	9272
p-FoxO1 (Ser256)	1:1000	Cell Signaling Technology	84192
p-mTOR (Ser2448)	1:1000	Cell Signaling Technology	2971
p-PRAS40 (Thr246)	1:1000	Cell Signaling Technology	2997
Acetyl-CoA carboxylase	1:1000	Cell Signaling Technology	3676
FASN	1:1000	Cell Signaling Technology	3180
p-4E-BP1 (Ser65)	1:1000	Cell Signaling Technology	9451
p-4E-BP1 (Thr37/46)	1:2000	Cell Signaling Technology	2855
4E-BP1	1:2000	Cell Signaling Technology	9644
p-S6 ribosomal protein (Ser235/236)	1:2000	Cell Signaling Technology	4858
p-AMPKα1 (Ser485)	1:1000	Cell Signaling Technology	2537
p-p44/42 MAPK (Erk1/2) (Thr202/Tyr204)	1:1000	Cell Signaling Technology	4370
p44/42 MAPK (Erk1/2)	1:1000	Cell Signaling Technology	9102
PCNA	1:1000	Cell Signaling Technology	2586
Cyclin D antibody	1:1000	Millipore	06-137
GAPDH	1:5000	Millipore	MAB374

4E-BP1, eukaryotic translation initiation factor 4E-binding protein 1; AKT, serine/threonine kinase; AMPK, 5'adenosine monophosphate–activated protein kinase; FASN, fatty acid synthase; FoxO1, forkhead box protein O1; GAPHD, glyceraldehyde-3-phosphate dehydrogenase; MAPK, mitogen-activated protein kinase; mTOR, the mammalian target of rapamycin; p-, phosphorylated; PCNA, proliferating cell nuclear antigen; RAS40, the proline-rich Akt substrate of 40 kDa.

to Entrez ID using the Bioconductor Package Maintainer org.Mm.eg.db version 3.8.2 (Bioconductor, Buffalo, NY; *https://www.bioconductor.org*). Duplicated and unannotated genes were removed. Data were filtered with counts per million >0.1 in at least two libraries. Normalized data were obtained by subtracting WT or KO data of 2D and 4D with 0D data relatively. The Edge R package version 3.28.1 (Bioconductor) was used to normalize data, calculate fragments per kilogram of exon model per million reads mapped, draw multidimensional scaling plot, and conduct KEGG pathway analysis. Heatmap was generated by Complexheatmap. Other plots was drawn with ggplot2 (R Foundation for Statistical Computing, Vienna, Austria).[29]

Statistical Analysis

Prism software version 6.0 (GraphPad, San Diego, CA) was applied to analyze the data, which are presented as means ± SD. Comparisons between two groups were performed with the two-tailed unpaired *t*-test. Survival curves were compared by the log-rank *t*-test. $P < 0.05$ was considered statistically significant.

Results

Activation of mTORC2 Signaling after PHx in Mice

To investigate the functional contribution of mTORC2 signaling on liver regeneration, two-thirds PHx was performed in 8-week–old male WT mice (in the C57BL/6 genetic background). Because mTORC2 is responsible for phosphorylation of Akt at the Ser473 site [p-Akt (S473)], expression levels of mTORC2 signaling were determined by Western blot analysis for the expression of p-Akt (S473) during PHx (Figure 1A). The upregulation of p-Akt (S473) was observed from day 2 after PHx. The relative p-Akt expression was quantified by calculating the p-Akt (S473) to total Akt ratio. p-Akt (S473) levels peaked at 2 to 3 days and returned to the baseline levels at 5 days after PHx (Figure 1B). An increased expression of phosphorylated Rps6 (p-Rps6) expression was also observed (Figure 1A). The expression of phosphorylated Foxo1 (p-Foxo1), phosphorylated 4E-bp1 (p-4E-bp1), phosphorylated Ampk (p-Ampk), and phosphorylated Erk (p-Erk) did not significantly change during PHx (Figure 1A). Altogether, these results indicate the activation of mTORC2 signaling along liver regeneration after PHx.

mTORC2 Deficiency in the Liver Does Not Affect Liver Development or Hepatocyte Polyploidy

Because Rictor is the unique component of mTORC2 complex,[13] the function of mTORC2 can be abolished by the deletion of *Rictor*. By crossing *Albumin-Cre* mice with $Rictor^{fl/fl}$ mice (all in the C57BL/6 background), $Rictor^{LKO}$ mice were generated. Before subsequent experiments, genotyping was performed to validate depletion of *Rictor* in these mice (Supplemental Figure S1A). The detailed metabolic phenotype of $Rictor^{LKO}$ mice has been previously described; specifically, it has been reported that loss of mTORC2 in the liver results in impaired glycolysis and lipogenesis on insulin stimulation or feeding, whereas otherwise these mice are rather healthy.[30–32] Similar to previous reports,[30,31] $Rictor^{LKO}$ mice were born at Mendelian ratio and developed normally. At 3 weeks of age, the

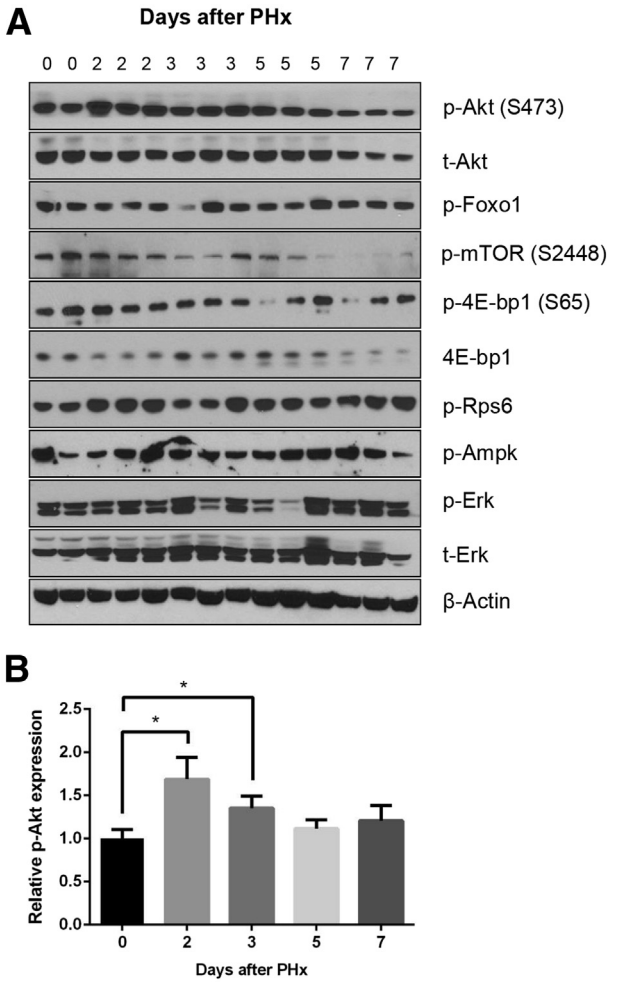

Figure 1 Liver mammalian target of rapamycin (mTOR) complex 2 pathway is activated after partial hepatectomy. **A:** Western blot analysis of indicated proteins in livers lysates from wild-type mice before (0 days) and after partial hepatectomy (PHx) (2 to 7 days). **B:** The densitometry analysis of the ratio of p-Akt (S473) to t-Akt is shown in wild-type mice before and after PHx. $*P < 0.05$. p-, phosphorylated; t-, total.

liver was similar in all aspects in *Rictor*$^{fl/fl}$ mice and *Rictor*^{LKO} mice (Supplemental Figure S1, B–E). However, ablation of *Rictor* in the mouse liver resulted in a slight decrease in liver weight as well as liver weight to body weight ratio in 5-week–old mice (Supplemental Figure S2). Histologically, a significant reduction of hepatocyte area was observed in *Rictor*^{LKO} mice (Supplemental Figure S2). However, there was no significant difference in Ki-67–positive cells in liver tissues from WT *Rictor*$^{fl/fl}$ mice and *Rictor*^{LKO} littermates (Supplemental Figures S2). These phenotypes were also preserved in 8-week–old adult mice (Supplemental Figure S3). Meanwhile, no spontaneous hepatic apoptosis, necroptosis, or necrosis was observed in the liver tissues from *Rictor*$^{fl/fl}$ mice and *Rictor*^{LKO} mice (Supplemental Figures S3). The phenotypes observed here were similar to those that have been reported previously.[30] The decreased hepatocyte area was due to the decreased glycogen and triglyceride storage in the *Rictor*^{LKO} liver.

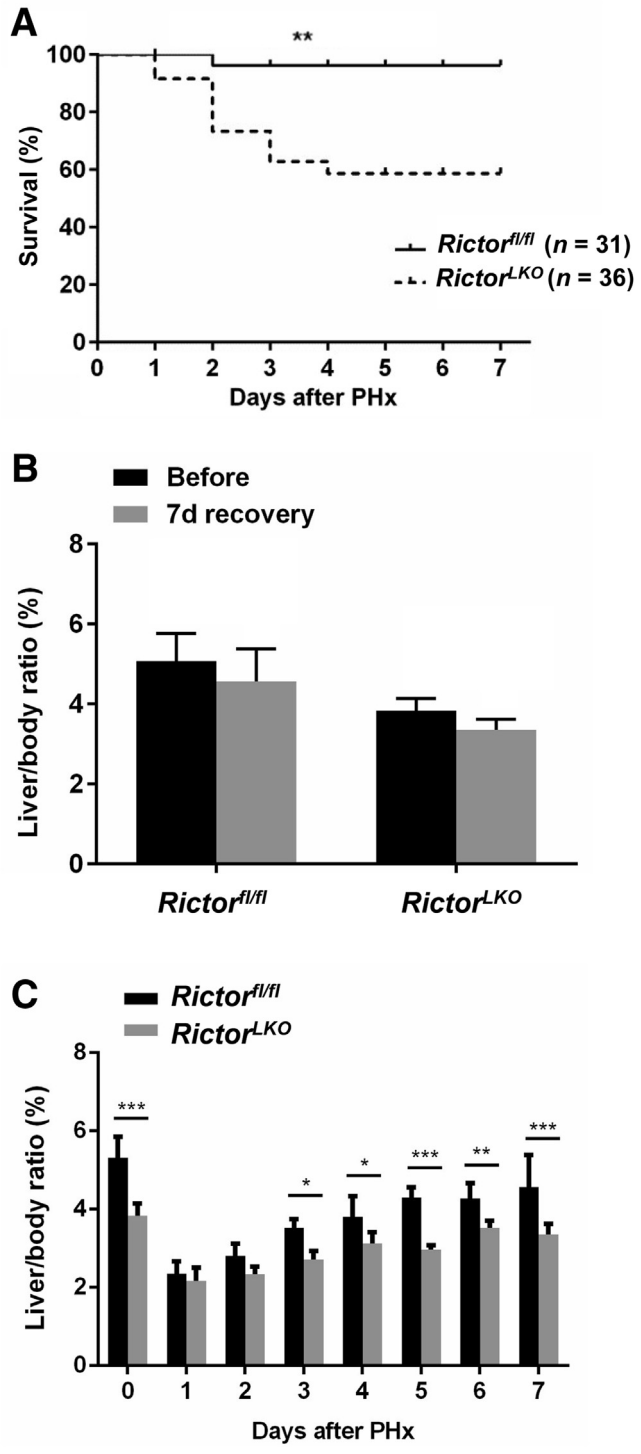

Figure 2 Liver-specific deletion of *Rictor* increases mouse mortality after partial hepatectomy (PHx). **A:** Survival curves from *Rictor* wild-type (*Rictor*$^{fl/fl}$) and *Rictor* knockout (*Rictor*^{LKO}) mice after PHx. **B:** Liver weight and liver/body ratio of *Rictor*$^{fl/fl}$ and *Rictor*^{LKO} mice before and 7 days after PHx. **C:** Liver weight and liver/body ratio of *Rictor*$^{fl/fl}$ and *Rictor*^{LKO} mice at 0 to 7 days after PHx. $n = 31$ *Rictor*$^{fl/fl}$ mice (**A**); $n = 36$ *Rictor*^{LKO} mice (**A**); $n = 6$ *Rictor*$^{fl/fl}$ mice (**B**); $n = 5$ *Rictor*^{LKO} (**B**); $n = 3$ *Rictor*$^{fl/fl}$ mice (**C**); $n = 4$ *Rictor*^{LKO} mice (**C**). $*P < 0.05$, $**P < 0.01$, and $***P < 0.001$ versus *Rictor*^{LKO}(Kaplan-Meier log rank test).

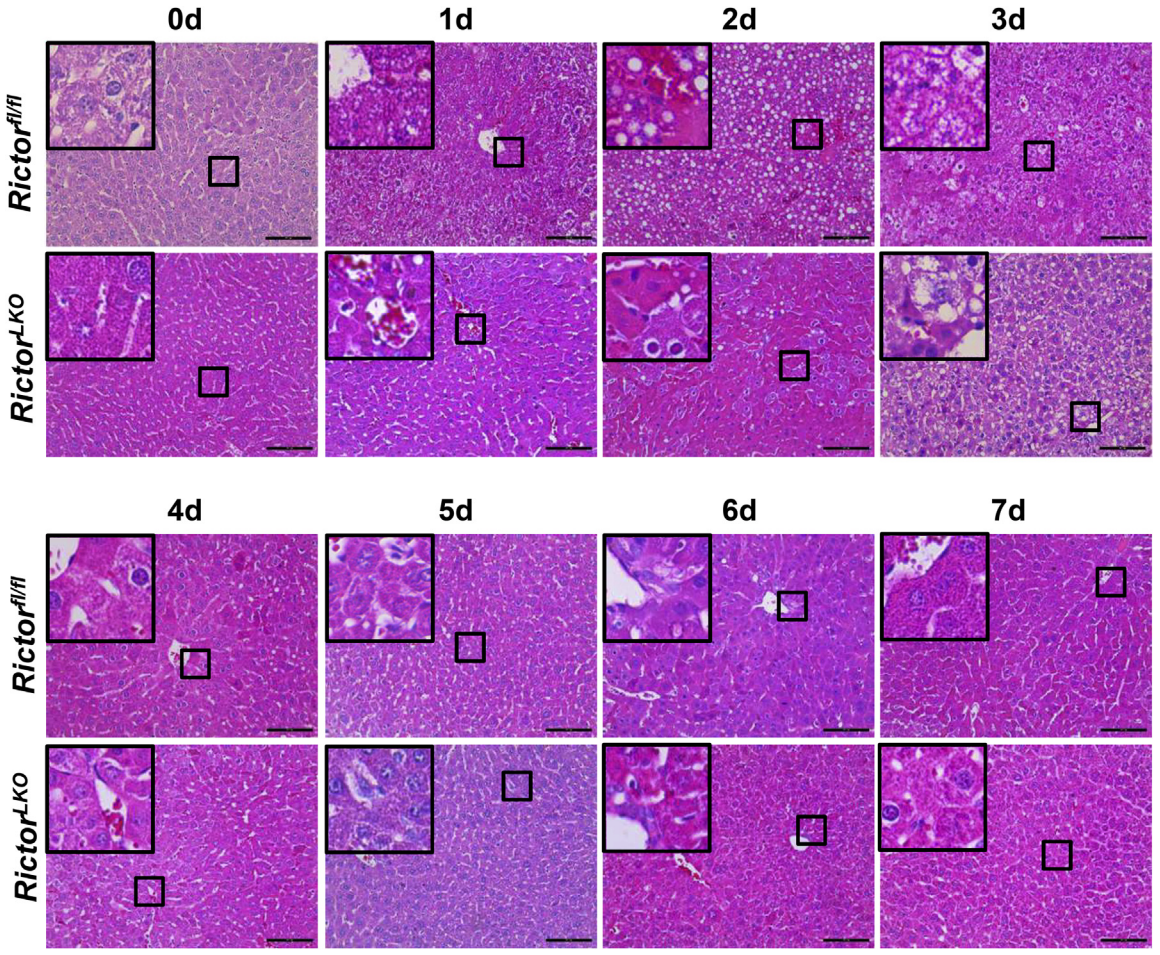

Figure 3 Histologic analysis of mouse livers in response to partial hepatectomy. Representative hematoxylin and eosin–stained sections of livers isolated from *Rictor* wild-type (*Rictor*$^{fl/fl}$) and *Rictor* knockout (*Rictor*^{LKO}) mice before (0 days) and after partial hepatectomy (1 to 7 days). **Boxed areas** are shown at higher magnification in the **insets**. Original magnification: × 100 (**main images**); ×370 (**insets**). Scale bars = 200 μm.

Indeed, in fasting state, there was no difference in liver weight and liver/body ratio between *Rictor*$^{fl/fl}$ and *Rictor*^{LKO} mice (Supplemental Figures S4).

Hepatocytes are reported to be highly polyploid, which might influence how they function. Hepatocyte ploidies were analyzed using primary hepatocytes isolated from *Rictor*$^{fl/fl}$ mice and *Rictor*^{LKO} mice. The hepatocytes from the two cohorts of mice demonstrated similar ploidies (Supplemental Figure S5). In summary, these results are consistent with previous reports that mTORC2 is dispensable for normal liver development[32] and loss of mTORC2 does not affect liver homeostasis or hepatocyte ploidies.

mTORC2 Is Required for Liver Regeneration

Liver-specific *Akt1/2* KO in mice has been reported to impair liver regeneration and increase mortality after PHx.[22] We hypothesized that loss of mTORC2, which resulted in the impairment of Akt activities, would recapitulate these phenotypes after PHx. To test this hypothesis, PHx was performed in *Rictor*$^{fl/fl}$ and *Rictor*^{LKO} mice. *Rictor*-deficient mice were found to be more intolerant to PHx and exhibited decreased survival probability compared with their WT littermates (Figure 2A). Several *Rictor*^{LKO} mice died from day 1 to day 4 after PHx, and the remaining mice survived (Figure 2A). After 7 days of recovery, the liver weight/body weight ratio showed no difference in the two mouse cohorts before and after PHx, suggesting that all surviving mice were able to fully recover in terms of liver regeneration (Figure 2B). Although the liver/body weight ratio was similar in *Rictor*$^{fl/fl}$ and *Rictor*^{LKO} mice at 1 day after PHx, liver/body weight ratio recovered at a slower pace in *Rictor*^{LKO} mice when compared with their WT littermates (Figure 2C). Grossly, the enlargement in liver mass was evident during liver regeneration from day 0 to day 7 after PHx (Supplemental Figures S6–S13). Histologically, comparisons between two groups were conducted by hematoxylin and eosin staining (Figure 3 and Supplemental Figures S6–S13). Inflammatory responses could be observed in both groups at day 1 to day 3 after PHx. Increased vacuolization areas accumulated at day 2 and day 3 in *Rictor*$^{fl/fl}$ mice compared with *Rictor*^{LKO} mice (Figure 3 and Supplemental Figures S8 and S9).

Subsequently, a series of serum biochemical markers were analyzed to evaluate liver functions among *Rictor*$^{fl/fl}$

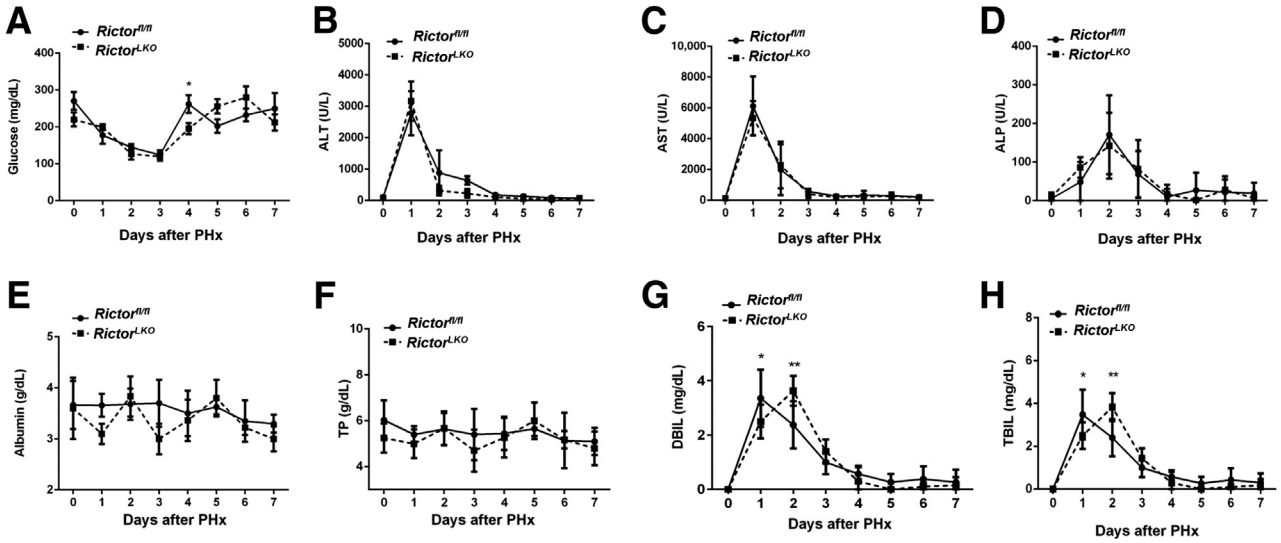

Figure 4 *Rictor* deficiency in mouse liver does not significantly affect serum biochemical markers during liver regeneration. Blood glucose (**A**), serum alanine transaminase (ALT) (**B**), aspartate transaminase (AST) (**C**), alkaline phosphatase (ALP) (**D**), albumin (**E**), total protein (TP) (**F**), direct bilirubin (DBil) (**G**), and total bilirubin (TBil) (**H**) levels are shown. $*P < 0.05$, $**P < 0.01$ $Rictor^{fl/fl}$ versus $Rictor^{LKO}$ at the same time point.

and $Rictor^{LKO}$ mice after PHx. No remarkable change of blood glucose levels during liver regeneration from day 0 to day 7 after PHx was detected (Figure 4A). Liver injury—related serum markers, such as alanine transaminase, aspartate transaminase, and alkaline phosphatase, markedly increased at day 1 after PHx and subsequently returned to normal, with no significant difference between the two groups of mice at each time point (Figure 4, B—D). Furthermore, no remarkable change of albumin and total protein levels was detected during liver regeneration (Figure 4, E and F). Interestingly, serum levels of direct bilirubin and total bilirubin peaked at day 1 after PHx in $Rictor^{fl/fl}$ mice, whereas serum levels of direct bilirubin and total bilirubin peaked at day 2 after PHx in $Rictor^{LKO}$ mice (Figure 4, G and H), consistent with a delayed regeneration in $Rictor^{LKO}$ mice. In summary, the present results indicated that loss of mTORC2 delays liver regeneration after PHx. The overall phenotype is similar to that observed in liver-specific *Akt1/2 KO* mice.

mTORC2 Deficiency Delays Hepatocyte Proliferation and Lipid Biosynthesis

To elucidate the potential mechanisms responsible for the observed events, the hepatocyte proliferation rate was studied after PHx between $Rictor^{fl/fl}$ and $Rictor^{LKO}$ mice by immunohistochemical staining of Ki-67 and PH3, two markers of proliferation. The percentage of Ki-67—positive cells markedly increased at day 1 and day 2 after PHx in $Rictor^{fl/fl}$ mice and decreased from day 3 after PHx. In contrast, the percentage of Ki-67—positive cells slightly increased to reach a peak at day 3 and then slowly decreased until day 7 after PHx in $Rictor^{LKO}$ mice (Figure 5, A and B, and Supplemental Figures S6—S13). A similar trend was also observed in terms of the percentage of PH3-positive cells, showing that proliferative cells burst out during the first 2 days after PHx and markedly decreased in $Rictor^{fl/fl}$ mice, while the cells maintained a slow but relatively moderate level in $Rictor^{LKO}$ mice (Figure 5C and Supplemental Figures S6—S13). Consistent with the delayed peaks of proliferation markers, delay in the lipid accumulation was also found in $Rictor^{LKO}$ mice after PHx (Figure 6). Taken together, these results indicate that mTORC2 affects cell proliferation and lipid formation during liver regeneration.

mTORC2 Modulates Liver Regeneration via Regulation of Cell Cycle and Lipid Accumulation

Next, the molecular differences between $Rictor^{fl/fl}$ and $Rictor^{LKO}$ mice were studied after PHx. The major signaling cascades involved in liver regeneration were investigated at the baseline and 1 day, 2 days, and 4 days after PHx using Western blotting analysis (Figure 7).

Because Akt is a major substrate of mTORC2, deletion of *Rictor* was accompanied by down-regulation of p-Akt (S473). Moreover, levels of p-Foxo1, p-Rps6, p-4E-bp1(S65), and p-4E-bp1 (T37/46) were also lower in $Rictor^{LKO}$ mice at the baseline level (Figure 7A). Genes involved in hepatocyte proliferation (Ccnd1 and Pcna) and lipogenesis (Fasn, Acc and p-Ampk) were expressed at similar levels in $Rictor^{fl/fl}$ and $Rictor^{LKO}$ mice (Figure 7A).

At day 1 after PHx (Figure 7B), expression of p-Akt (S473) markedly increased in $Rictor^{fl/fl}$ mice, whereas it remained at low levels in $Rictor^{LKO}$ mice. However, expression of p-Rps6, p-4E-bp1(S65), and p-4E-bp1 (T37/46) was similar in the two cohorts of mice. Unexpectedly, p-FoxO1 was upregulated in $Rictor^{LKO}$ mice when compared with $Rictor^{fl/fl}$ mice. Although the expression of hepatocyte

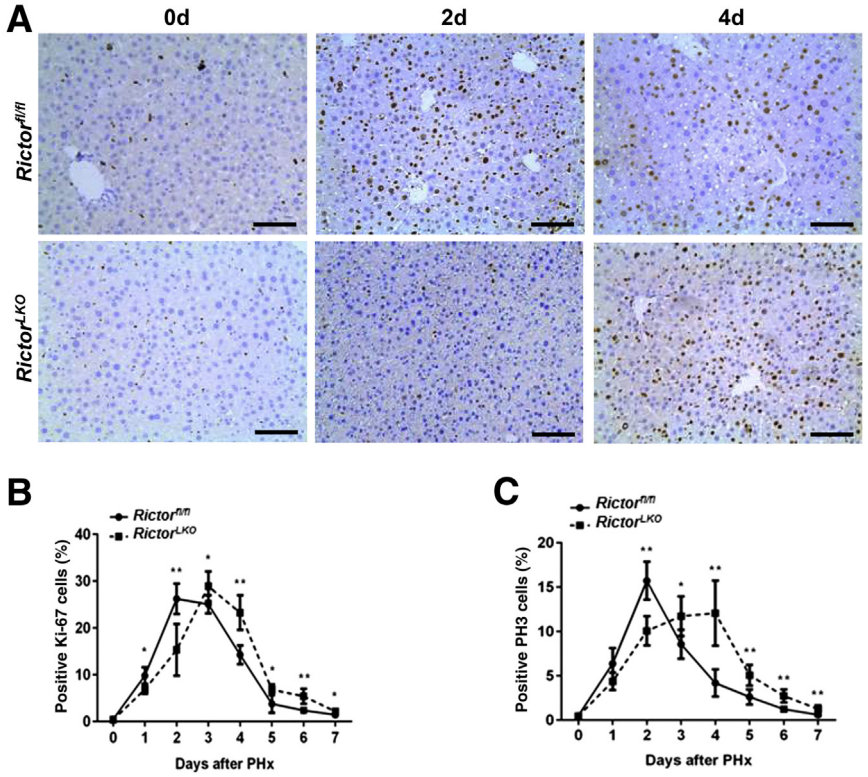

Figure 5 Delayed cell proliferation characterizes *Rictor*-deficient regenerative livers. **A:** Representative Ki-67 staining images in *Rictor* wild-type (*Rictor*$^{fl/fl}$) and *Rictor* knockout (*Rictor*^{LKO}) mice livers 0 day (0d), 2 days (2d), and 4 days (4d) after partial hepatectomy (PHx). **B:** Quantification of positive Ki-67 nuclei/total nuclei at different time points in *Rictor*$^{fl/fl}$ and *Rictor*^{LKO} mice livers before and after PHx. **C:** Quantification of positive phosphorylated histone 3 (PH3) nuclei/total nuclei at different time points in *Rictor*$^{fl/fl}$ and *Rictor*^{LKO} mice before and after PHx. $*P < 0.05$, $**P < 0.01$ *Rictor*$^{fl/fl}$ versus *Rictor*^{LKO} at the same time point. Original magnification, ×200. Scale bars = 100 μm.

proliferation genes, *Ccnd1* and *Pcna*, was similar in these mice, the expression of lipogenic pathway genes, including *Fasn* and *Acc*, was slightly lower in *Rictor*^{LKO} mice at this time point. At day 2 after PHx (Figure 7C), expression of p-Akt (S473) remained at low levels in *Rictor*^{LKO} mice. Expression of p-Rps6, p-4E-bp1(S65), p-4E-bp1 (T37/46), and p-Foxo1, as well as *Ccnd1* and *Pcna*, was similar to what have been observed in day 1 among *Rictor*$^{fl/fl}$ mice and *Rictor*^{LKO} mice. This finding coincided with the delay in lipid droplet accumulation during PHx in *Rictor*^{LKO} mice at

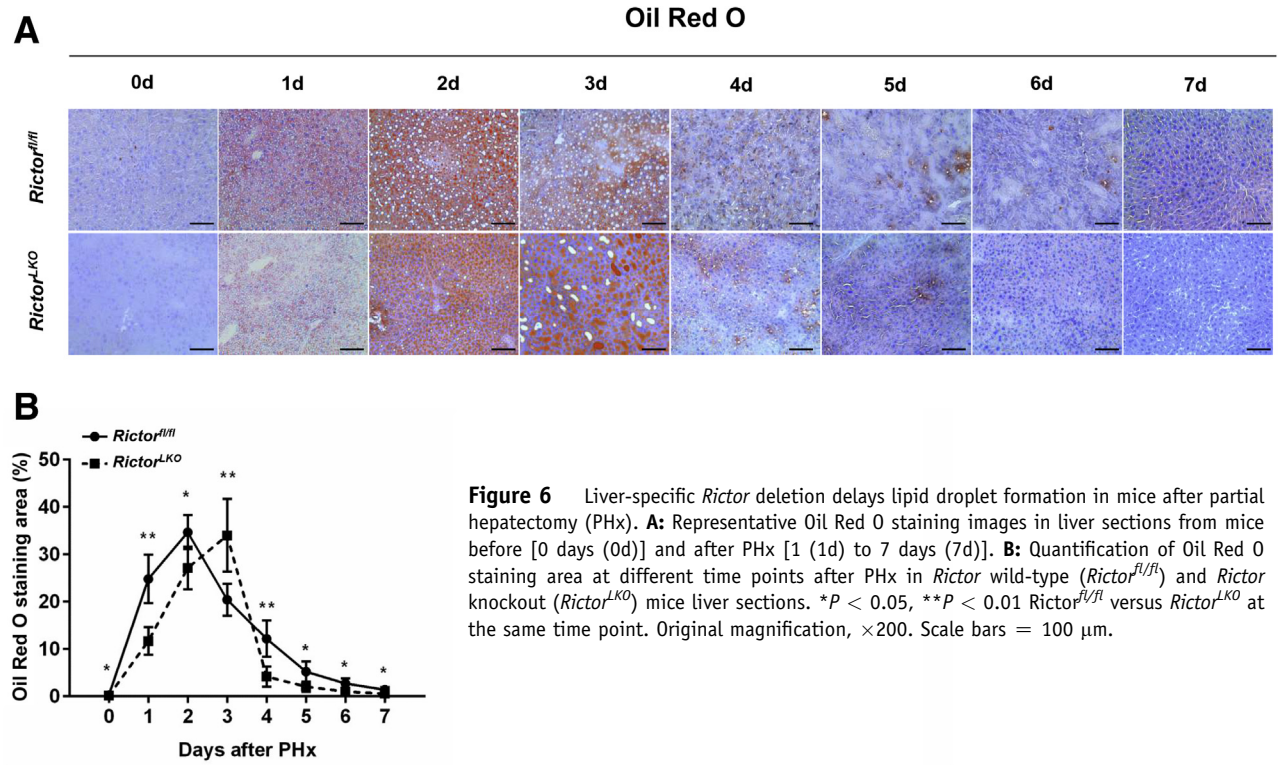

Figure 6 Liver-specific *Rictor* deletion delays lipid droplet formation in mice after partial hepatectomy (PHx). **A:** Representative Oil Red O staining images in liver sections from mice before [0 days (0d)] and after PHx [1 (1d) to 7 days (7d)]. **B:** Quantification of Oil Red O staining area at different time points after PHx in *Rictor* wild-type (*Rictor*$^{fl/fl}$) and *Rictor* knockout (*Rictor*^{LKO}) mice liver sections. $*P < 0.05$, $**P < 0.01$ Rictor$^{fl/fl}$ versus *Rictor*^{LKO} at the same time point. Original magnification, ×200. Scale bars = 100 μm.

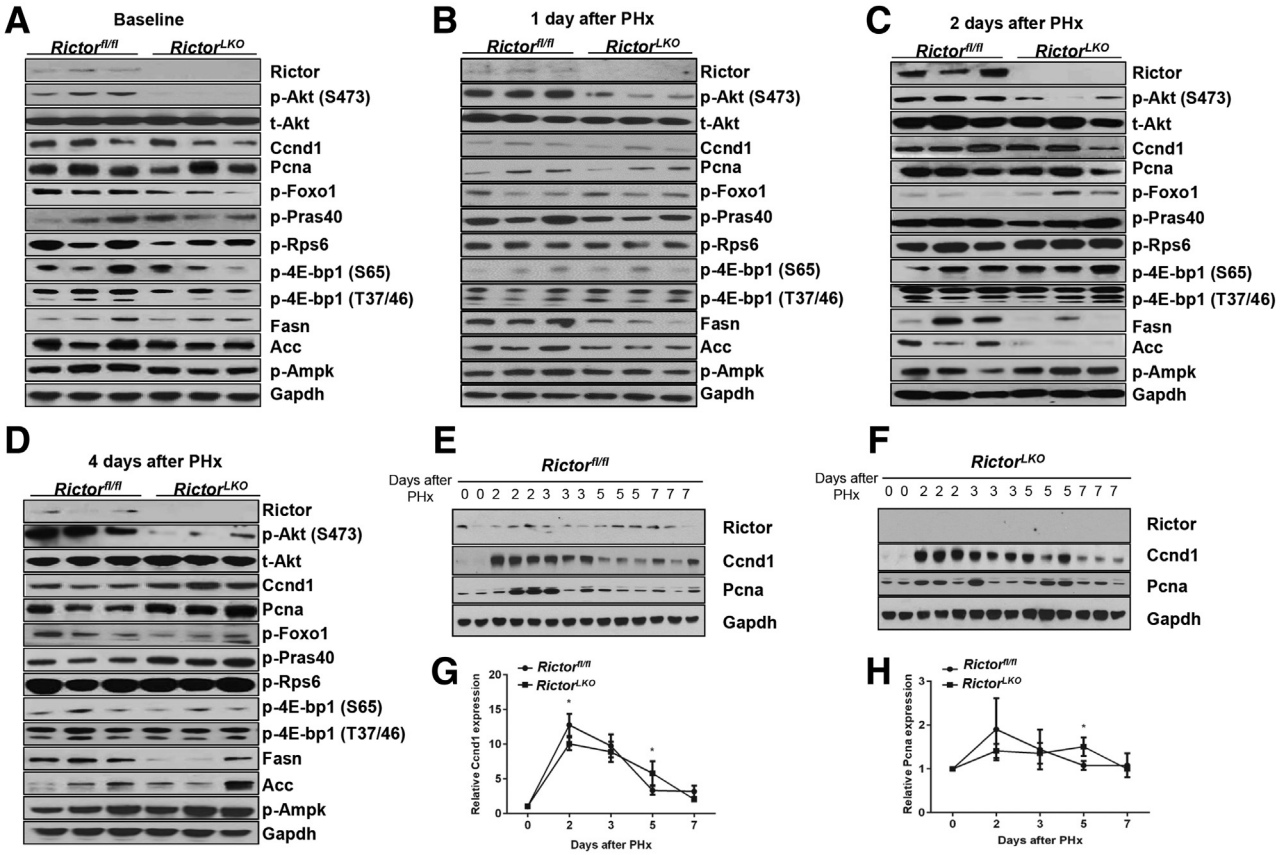

Figure 7 Delayed expression of Ccnd1 and Pcna in Rictor-deficient regenerative livers. **A**–**D:** Western blot analysis of indicated proteins in livers lysates from *Rictor* wild-type (*Rictor*$^{fl/fl}$) and *Rictor* knockout (*Rictor*^{LKO}) mice 0 day (**A**), 1 day (**B**), 2 days (**C**), and 4 days (**D**) after partial hepatectomy. **E** and **F:** Western blot analysis of indicated proteins at different time points in *Rictor*$^{fl/fl}$ and *Rictor*^{LKO} mouse livers before and after PHx. **G** and **H:** Densitometry analysis of hepatic Ccnd1 (**G**) and Pcna (**H**) expression at different time points in *Rictor*$^{fl/fl}$ and *Rictor*^{LKO} mice livers before and after PHx. $^*P < 0.05$ Rictor$^{fl/fl}$ versus Rictor^{LKO} at the same time point.

this time point. At 4 days after PHx (Figure 7D), a recovery of *Fasn* and *Acc1* levels was seen in *Rictor*^{LKO} mice. Intriguingly, the expression of Ccnd1 and Pcna was higher in *Rictor*^{LKO} mice than that detected in *Rictor*$^{fl/fl}$ mice.

Because delayed yet sustained hepatocyte proliferation was a major cellular phenotype in *Rictor*^{LKO} mice after PHx (Figure 5), the detailed time course analysis of *Ccnd1* and *Pcna* expression was performed in *Rictor*$^{fl/fl}$ and *Rictor*^{LKO} mice after PHx (Figure 7, E and F). *Ccnd1* was expressed at higher levels in *Rictor*$^{fl/fl}$ mice than in *Rictor*^{LKO} mice at 2 days after PHx. In addition, although *Ccnd1* and *Pcna* levels returned to the baseline levels at 5 days PHx in *Rictor*$^{fl/fl}$ mice, they remained higher in *Rictor*^{LKO} mice (Figure 7, G and H). Thus, the present findings imply a critical regulatory function of mTORC2 on hepatocyte proliferation during liver regeneration.

Global RNA Sequencing Confirms the Role of mTORC2 Signaling in Regulating Cell Proliferation and Metabolism during Liver Regeneration

To further investigate the pathways regulated by mTORC2 during liver regeneration after PHx, RNA sequencing analysis of liver tissues was performed from *Rictor*$^{fl/fl}$ and *Rictor*^{LKO} mice at 0 day (baseline), 2 days, and 4 days after PHx. Multidimensional scaling plot revealed relatively closer gene expression patterns of *Rictor*$^{fl/fl}$ and *Rictor*^{LKO} mouse liver at day 0. PHx promoted significant gene expression changes in the liver. It is clear, however, that the global gene expression patterns at day 4 are closer to day 0 in *Rictor*$^{fl/fl}$ mice but not in *Rictor*^{LKO} mice (Figure 8A). These results provide unbiased evidence that liver tissues are returning to their baseline state at day 4 in *Rictor*$^{fl/fl}$ mice but not in *Rictor*^{LKO} mice. Because the delayed cell cycle progression is a major phenotype observed in *Rictor*^{LKO} mice, the major cell cycle regulators, including *Ccnd1*, *Ccne1*, *Cdk4*, *Mdm2*, and *p27*, were analyzed based on the RNA sequencing data. *Ccnd1*, *Ccne1*, *Cdk4*, and *Mdm2* were expressed at high levels at day 2 in *Rictor*$^{fl/fl}$ mice, and their expression levels were lower at day 4 after PHx than those seen in day 2 after PHx. In contrast, in *Rictor*^{LKO} mice, these genes remained at higher levels at day 4 after PHx (Figure 8, B–E). The expression of *Cdkn1d* or *p27*, a cell cycle inhibitor, was significantly downregulated at day 2 after PHx, and it returned to the level close to the baseline

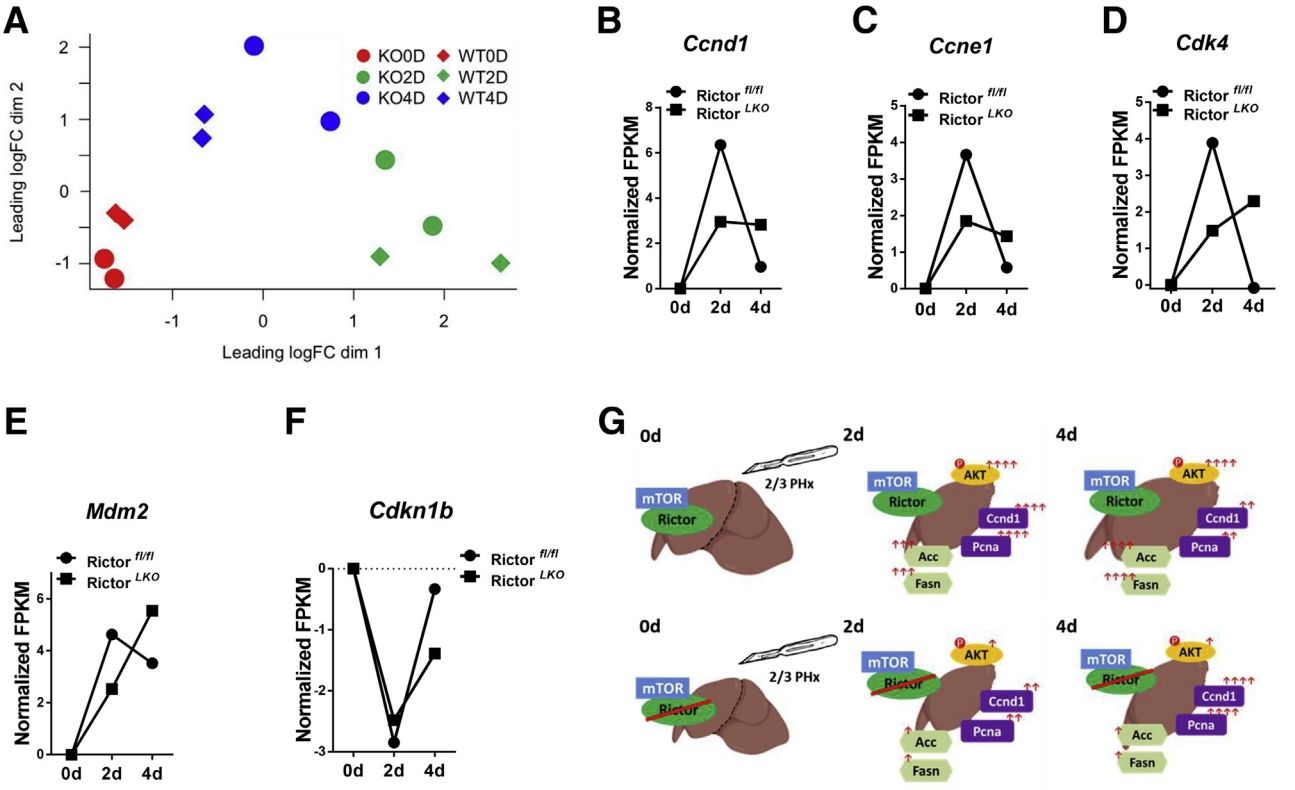

Figure 8 RNA sequencing results show mammalian target of rapamycin (mTOR) complex 2 signaling regulating cell proliferation and metabolism. **A:** Multidimensional scaling plot of the global gene expression patterns of 0 day (0D), 2 days (2D), and 4 days (4D) after partial hepatectomy (PHx) in *Rictor* wild-type (*Rictor*$^{fl/fl}$) and *Rictor* knockout (*Rictor*^{LKO}) mice. **B**–**F:** Normalized fragments per kilogram of exon model per million reads mapped (FPKM) of indicated gene (*Ccnd1*, *Ccne1*, *Cdk4*, *Mdm2*, and *Ckdn1b*) expression at 0d, 2d, and 4d after PHx in *Rictor*$^{fl/fl}$ and *Rictor*^{LKO} mice. Dotted line indicates normalized FPKM value equals to 0. **G:** Graphical abstract for the study.

at day 4 after PHx in *Rictor*$^{fl/fl}$ mice. In *Rictor*^{LKO} mice, *p27* expression remained at a low level at day 4 after PHx (Figure 8F). In addition, KEGG pathway analysis was performed for genes differently expressed on day 0, day 2, or day 4 in *Rictor*$^{fl/fl}$ and *Rictor*^{LKO} mouse liver tissues. Multiple pathways were found to be deregulated when mTORC2 was deleted at baseline levels as well as during liver regeneration after PHx (Supplemental Figures S14–S16). Overall, the RNA sequencing studies provide unbiased evidence and confirm that the loss of mTORC2 leads to a delayed liver regeneration after PHx.

Discussion

With increased understanding of the biological mechanisms underlying liver regeneration, the clinical practice for curing liver diseases has improved enormously during the past decades. However, there are still challenges for more aggressive surgical resections in the setting of malignancy due to predamaged liver functions and improper regenerative processes. Thus, liver transplantation is the last choice for surgical treatment in addition to palliative treatments.[33] A successful liver transplantation calls for providing an adequately sized, functioning graft for the recipient as well as maintaining a high safety profile for the donor. Complications, such as small transplantation and recipients' liver failure, still happen frequently.[34] The trade-off between removal and retention remains the major challenge for surgeons. Thus, a better understanding of liver regeneration may shed light on clinical treatment strategies and availability of high-quality transplantable organs.

Numerous complex and interconnected signaling pathways have been uncovered to be involved in liver regeneration.[35] mTOR signaling has been validated to be essential for regulating organismal growth, development, proliferation, and viability in response to nutrient availability.[36] The mTOR kinase is considered to be a master regulator of growth that functions in two distinct complexes: mTORC1 (defined by the Raptor subunit) and mTORC2 (defined by the Rictor subunit).[36] Although much is known about the inputs, outputs, and regulatory features of mTORC1, mTORC2 regulation and function remain poorly understood. In the present study, we investigated the functional role of mTORC2 during liver regeneration after PHx using *Rictor*^{LKO} mice. The results show that mTORC2 signaling is activated after PHx (Figure 1) and liver-specific deletion of *Rictor* causes significant early-stage mortality after PHx

(Figure 2A). The data obtained in this study are similar to those observed in liver-specific *Akt1/Akt2* double KO mice. Indeed, approximately 40% of *Akt1/Akt2* KO mice did not survive after the PHx.[22] These findings are consistent with the fact that Akt kinases are considered to be the major substrates of mTORC2. Previous studies have found that Pi3k and Pdk1 pathways are required for liver regeneration.[17,37] Our data therefore add additional evidence to support the major role of the PI3k/Akt signaling cascade during this important physiologic process.

Mechanistically, we discovered that mTORC2 regulates hepatocyte proliferation and lipid accumulation after PHx, which is reflected by the delayed peak of Ki-67 and PH3 immunostaining as well as Oil Red O staining in $Rictor^{LKO}$ mice. Consistently, at the biochemical levels, we found that the lipogenic pathway genes *Fasn* and *Acc* are expressed at lower levels at 2 days after PHx and higher expression of the cell proliferation genes *Ccnd1* and *Pcna* in $Rictor^{LKO}$ mice is seen at 4 days after PHx (Figure 8G). We compared our data with that reported in *Akt1/2* double KO mice by Pauta et al,[22] who found that WT mice exhibit significant lipid droplet accumulation at 2 to 4 days after PHx. The observation is consistent with our results. In contrast, *Akt1/2* double KO mice failed to accumulate lipid droplets after PHx. This phenotype is different from that of $Rictor^{LKO}$ mice. In $Rictor^{LKO}$ mice, lipid droplet accumulation was delayed but not abolished. Of note, either deletion of *Akt1/2* or ablation of mTORC2 was found to cause early-stage mortality after PHx. Our PHx surgery was performed by one expert researcher (H.W.), thus ruling out the possibility that the early mortality observed in $Rictor^{LKO}$ mice was due to a surgical technique issue. The precise mechanisms leading to the higher mortality in $Rictor^{LKO}$ mice or liver-specific *Akt1/2* double KO mice remain to be determined. It was previously reported that there was severe hypoglycemia 12 hours after PHx in *Akt1/2* KO mice, suggesting that this metabolic defect might be the major cause of the early death during PHx in these mice.[22] The blood glucose levels in control and $Rictor^{LKO}$ mice was analyzed at 24 hours after PHx, and the two cohorts of mice demonstrated the similar blood glucose levels (Figure 4A). Notably, the blood was collected from the surviving mice, and the possibility that those dead mice might have hypoglycemia cannot be ruled out. Clearly, additional studies are required to further investigate this issue. Regarding the hepatocyte proliferation, Pauta et al[22] found that in WT mice, hepatocyte proliferation peaked at 2 days after PHx, decreased at 4 days, and returned to the baseline levels at 6 days. In *Akt1/2* double KO mice, hepatocyte proliferation was lower throughout the time after PHx. Intriguingly, $Rictor^{LKO}$ mice had delayed but more sustained hepatocyte proliferation after PHx. Overall, the molecular phenotypes are milder in $Rictor^{LKO}$ mice than those seen in *Akt1/2* double KO mice. The data are consistent with the finding that Akt1/2 kinase activities are regulated by multiple factors, and mTORC2 is one of the major complexes in this regulatory network.[38] Loss of mTORC2 significantly decreased Akt1/2 activity, presumably without abolishing it. In addition, male mice were used in these studies for a better head to head comparison with studies by Pauta et al[22] between roles of Akt1/2 and mTORC2 during liver regeneration. Although we do not expect sex difference in terms of mTORC2 regulation of liver regeneration, expanded studies with both male and female mice will be of great help to further substantiate our findings.

Using RNA sequencing analysis, we identified pathways that are differentially expressed in $Rictor^{fl/fl}$ and $Rictor^{LKO}$ mouse liver tissues at baseline levels (Supplemental Figure S14) as well as during regeneration (Supplemental Figures S15 and S16). As expected, metabolic regulating pathways, such as PI3K-Akt signaling pathways and galactose metabolism pathways, were downregulated in $Rictor^{LKO}$ mice at the baseline levels (Supplemental Figure S14). At day 2 after PHx, immunoregulatory signaling cascades, including Th17, Th1, and Th2 cell differentiation signaling and T-cell receptor signaling, were also significantly impaired in $Rictor^{LKO}$ mice, indicating immunosuppression during liver regeneration in the condition of mTORC2 deficiency (Supplemental Figure S15). At day 4 after PHx, transforming growth factor-β signaling pathway as well as signals in regulating mitophagy and autophagy were identified to be down-regulated in $Rictor^{LKO}$ mice, suggesting a potential cell proliferation brake occurring in WT mice for preventing liver overgrowth (Supplemental Figure S16). Furthermore, multiple metabolic cascades, especially fatty acid metabolic pathways, were deregulated in $Rictor^{LKO}$ mice at this time point. The data are consistent with the key roles of these metabolic events during liver regeneration. Hippo cascade is a major signal that regulates organ size and hepatocyte proliferation.[39] *Yap1*, *Wwtr1,* and *Tead1*, all key transcriptional factors downstream of Hippo kinases, were induced at higher levels in WT mice than those in $Rictor^{LKO}$ mice, especially at day 2 after PHx (Supplemental Figure S17). The result suggests that mTORC2 may function to regulate liver regeneration via Hippo cascade. Clearly, additional functional studies are required to further analyze the contribution of these pathways during liver regeneration.

Our investigation uncovers the role of mTORC2 in regulating hepatocyte proliferation and lipid metabolism. mTORC2/Akt cascade regulates multiple downstream signaling pathways, including Tsc/mTORC1 and FoxOs.[38,40] Tsc/mTORC1 in turns regulates p70S6k/Rps6 and 4E-bp1/Eif4e signaling pathways, which regulate lipogenesis and protein translation, respectively.[41] FoxO family members are transcriptional factors, which regulate cell proliferation, metabolism, and apoptosis. FoxO1 is considered to be the major FoxO isoform in the liver.[42] In *Akt1//2* double KO mice, it was found that concomitant ablation of *FoxO1* rescued the liver regeneration deficiency. The results suggest that FoxO1 may be the major molecule downstream of Akt during liver regeneration. However, the functional

contribution of Tsc/mTORC1 in liver regeneration downstream of Akt has not been determined. It would be of high importance to further investigate these two pathways in liver regeneration, hepatocyte proliferation, and lipogenesis downstream of mTORC2. The hypothesis should be tested by generating liver-specific *Tsc1/Rictor* KO mice (to allow the activation of mTORC1 in the absence of mTORC2) or liver specific *Foxo1/Rictor* double KO mice (to simultaneously delete *Foxo1* and mTORC2). The mice could be subjected to PHx, and the hepatocyte proliferation and lipogenesis after PHx could be evaluated. These studies would provide important information about the biochemical crosstalk among these pathways in PHx.

At the translational level, together with the studies by Pauta et al,[22] we demonstrate that mTORC2/AKT cascade is a major signaling pathway in modulating liver regeneration after PHx. This study suggests that strategies that maintain or increase the mTORC2/AKT pathway may be useful to accelerate liver regeneration. On the other hand, mTORC2 inhibitors or AKT inhibitors may lead to delayed liver regeneration in humans. Therefore, a critical consideration and well evaluation of liver function shall be applied before hepatectomy and mTORC2 inhibitor administration.

Acknowledgments

We thank the University of California, San Francisco Liver Center Cell Biology core for the assistance with primary mouse hepatocytes isolation; Parnassus Flow Cytometry Core (PFCC) for assistance in generating the flow cytometry data; and Congyu Xu for her professional help with R language.

Supplemental Data

Supplemental material for this article can be found at *http://doi.org/10.1016/j.ajpath.2019.12.010*.

References

1. Wolf JH, Holmes MV, Fouraschen S, Keating BJ, Baker T, Emond J, Rader DJ, Shaked A, Olthoff KM: Serum lipid expression correlates with function and regeneration following living donor liver transplantation. Liver Transpl 2016, 22:103−110
2. Corless JK, Middleton HM 3rd: Normal liver function: a basis for understanding hepatic disease. Arch Intern Med 1983, 143: 2291−2294
3. Riehle KJ, Dan YY, Campbell JS, Fausto N: New concepts in liver regeneration. J Gastroenterol Hepatol 2011, 26 Suppl 1:203−212
4. Michalopoulos GK: Hepatostat: liver regeneration and normal liver tissue maintenance. Hepatology 2017, 65:1384−1392
5. Michalopoulos GK, DeFrances MC: Liver regeneration. Science 1997, 276:60−66
6. Clavien PA, Petrowsky H, DeOliveira ML, Graf R: Strategies for safer liver surgery and partial liver transplantation. N Engl J Med 2007, 356:1545−1559
7. Forbes SJ, Newsome PN: Liver regeneration: mechanisms and models to clinical application. Nat Rev Gastroenterol Hepatol 2016, 13:473−485
8. Oh SH, Swiderska-Syn M, Jewell ML, Premont RT, Diehl AM: Liver regeneration requires Yap1-TGFbeta-dependent epithelial-mesenchymal transition in hepatocytes. J Hepatol 2018, 69:359−367
9. Kong B, Sun R, Huang M, Chow MD, Zhong XB, Xie W, Lee YH, Guo GL: Fibroblast growth factor 15-dependent and bile acid-independent promotion of liver regeneration in mice. Hepatology 2018, 68:1961−1976
10. Michalopoulos GK: Liver regeneration after partial hepatectomy: critical analysis of mechanistic dilemmas. Am J Pathol 2010, 176:2−13
11. Preziosi ME, Monga SP: Update on the mechanisms of liver regeneration. Semin Liver Dis 2017, 37:141−151
12. Panasyuk G, Patitucci C, Espeillac C, Pende M: The role of the mTOR pathway during liver regeneration and tumorigenesis. Ann Endocrinol (Paris) 2013, 74:121−122
13. Huang K, Fingar DC: Growing knowledge of the mTOR signaling network. Semin Cell Dev Biol 2014, 36:79−90
14. Wang Q, Yu WN, Chen X, Peng XD, Jeon SM, Birnbaum MJ, Guzman G, Hay N: Spontaneous hepatocellular carcinoma after the combined deletion of akt isoforms. Cancer Cell 2016, 29:523−535
15. Wei X, Luo L, Chen J: Roles of mTOR signaling in tissue regeneration. Cells 2019, 8:1075
16. Haga S, Ogawa W, Inoue H, Terui K, Ogino T, Igarashi R, Takeda K, Akira S, Enosawa S, Furukawa H, Todo S, Ozaki M: Compensatory recovery of liver mass by Akt-mediated hepatocellular hypertrophy in liver-specific STAT3-deficient mice. J Hepatol 2005, 43:799−807
17. Haga S, Ozaki M, Inoue H, Okamoto Y, Ogawa W, Takeda K, Akira S, Todo S: The survival pathways phosphatidylinositol-3 kinase (PI3-K)/phosphoinositide-dependent protein kinase 1 (PDK1)/Akt modulate liver regeneration through hepatocyte size rather than proliferation. Hepatology 2009, 49:204−214
18. Chen P, Yan H, Chen Y, He Z: The variation of AkT/TSC1-TSC1/mTOR signal pathway in hepatocytes after partial hepatectomy in rats. Exp Mol Pathol 2009, 86:101−107
19. Espeillac C, Mitchell C, Celton-Morizur S, Chauvin C, Koka V, Gillet C, Albrecht JH, Desdouets C, Pende M: S6 kinase 1 is required for rapamycin-sensitive liver proliferation after mouse hepatectomy. J Clin Invest 2011, 121:2821−2832
20. Jiang YP, Ballou LM, Lin RZ: Rapamycin-insensitive regulation of 4e-BP1 in regenerating rat liver. J Biol Chem 2001, 276:10943−10951
21. Palmes D, Zibert A, Budny T, Bahde R, Minin E, Kebschull L, Holzen J, Schmidt H, Spiegel HU: Impact of rapamycin on liver regeneration. Virchows Arch 2008, 452:545−557
22. Pauta M, Rotllan N, Fernandez-Hernando A, Langhi C, Ribera J, Lu M, Boix L, Bruix J, Jimenez W, Suarez Y, Ford DA, Baldan A, Birnbaum MJ, Morales-Ruiz M, Fernandez-Hernando C: Akt-mediated foxo1 inhibition is required for liver regeneration. Hepatology 2016, 63:1660−1674
23. Postic C, Shiota M, Niswender KD, Jetton TL, Chen Y, Moates JM, Shelton KD, Lindner J, Cherrington AD, Magnuson MA: Dual roles for glucokinase in glucose homeostasis as determined by liver and pancreatic beta cell-specific gene knock-outs using Cre recombinase. J Biol Chem 1999, 274:305−315
24. Magee JA, Ikenoue T, Nakada D, Lee JY, Guan KL, Morrison SJ: Temporal changes in PTEN and mTORC2 regulation of hematopoietic stem cell self-renewal and leukemia suppression. Cell Stem Cell 2012, 11:415−428
25. Mitchell C, Willenbring H: Addendum: a reproducible and well-tolerated method for 2/3 partial hepatectomy in mice. Nat Protoc 2014, 9:1532
26. Song X, Liu X, Wang H, Wang J, Qiao Y, Cigliano A, Utpatel K, Ribback S, Pilo MG, Serra M, Gordan JD: Combined CDK4/6 and pan-mTOR inhibition is synergistic against intrahepatic cholangiocarcinoma. Clin Cancer Res 2019, 25:403−413
27. Wang B, Zhao L, Fish M, Logan CY, Nusse R: Self-renewing diploid Axin2+ cells fuel homeostatic renewal of the liver. Nature 2015, 524: 180−185

28. Duncan AW, Taylor MH, Hickey RD, Newell AE, Lenzi ML, Olson SB, Finegold MJ, Grompe M: The ploidy conveyor of mature hepatocytes as a source of genetic variation. Nature 2010, 467:707
29. Roy M, Sorokina O, Skene N, Simonnet C, Mazzo F, Zwart R, Sher E, Smith C, Armstrong JD, Grant SG: Proteomic analysis of postsynaptic proteins in regions of the human neocortex. Nat Neurosci 2018, 21:130
30. Hagiwara A, Cornu M, Cybulski N, Polak P, Betz C, Trapani F, Terracciano L, Heim MH, Ruegg MA, Hall MN: Hepatic mTORC2 activates glycolysis and lipogenesis through Akt, glucokinase, and SREBP1c. Cell Metab 2012, 15:725−738
31. Yuan M, Pino E, Wu L, Kacergis M, Alexander A, Soukas: Identification of Akt-independent regulation of hepatic lipogenesis by mammalian target of rapamycin (mTOR) complex 2. J Biol Chem 2012, 287:29579−29588
32. Lamming DW, Demirkan G, Boylan JM, Mihaylova MM, Peng T, Ferreira J, Neretti N, Salomon A, Sabatini DM, Gruppuso PA: Hepatic signaling by the mechanistic target of rapamycin complex 2 (mTORC2). FASEB J 2014, 28:300−315
33. Meirelles Junior RF, Salvalaggio P, Rezende MB, Evangelista AS, Guardia BD, Matielo CE, Neves DB, Pandullo FL, Felga GE, Alves JA, Curvelo LA, Diaz LG, Rusi MB, Viveiros Mde M, Almeida MD, Pedroso PT, Rocco RA, Meira Filho SP: Liver transplantation: history, outcomes and perspectives. Einstein (Sao Paulo) 2015, 13:149−152
34. Lee SG: A complete treatment of adult living donor liver transplantation: a review of surgical technique and current challenges to expand indication of patients. Am J Transplant 2015, 15: 17−38
35. Valizadeh A, Majidinia M, Samadi-Kafil H, Yousefi M, Yousefi B: The roles of signaling pathways in liver repair and regeneration. J Cell Physiol 2019, 234:14966−14974
36. Laplante M, Sabatini DM: mTOR signaling in growth control and disease. Cell 2012, 149:274−293
37. Jackson LN, Larson SD, Silva SR, Rychahou PG, Chen LA, Qiu S, Rajaraman S, Evers BM: PI3K/Akt activation is critical for early hepatic regeneration after partial hepatectomy. Am J Physiol Gastrointest Liver Physiol 2008, 294:G1401−G1410
38. Dalle Pezze P, Sonntag AG, Thien A, Prentzell MT, Godel M, Fischer S, Neumann-Haefelin E, Huber TB, Baumeister R, Shanley DP, Thedieck K: A dynamic network model of mTOR signaling reveals TSC-independent mTORC2 regulation. Sci Signal 2012, 5:ra25
39. Patel SH, Camargo FD, Yimlamai D: Hippo signaling in the liver regulates organ size, cell fate, and carcinogenesis. Gastroenterology 2017, 152:533−545
40. Masui K, Tanaka K, Akhavan D, Babic I, Gini B, Matsutani T, Iwanami A, Liu F, Villa GR, Gu Y, Campos C, Zhu S, Yang H, Yong WH, Cloughesy TF, Mellinghoff IK, Cavenee WK, Shaw RJ, Mischel PS: mTOR complex 2 controls glycolytic metabolism in glioblastoma through FoxO acetylation and upregulation of c-Myc. Cell Metab 2013, 18:726−739
41. Wang C, Cigliano A, Jiang L, Li X, Fan B, Pilo MG, Liu Y, Gui B, Sini M, Smith JW, Dombrowski F, Calvisi DF, Evert M, Chen X: 4EBP1/eIF4E and p70S6K/RPS6 axes play critical and distinct roles in hepatocarcinogenesis driven by AKT and N-Ras proto-oncogenes in mice. Hepatology 2015, 61:200−213
42. Tikhanovich I, Cox J, Weinman SA: Forkhead box class O transcription factors in liver function and disease. J Gastroenterol Hepatol 2013, 28 Suppl 1:125−131